Contact Dynamics and Coupled Stability of Massage Compliant Robotic Arm With Impedance Controller

Yuancan Huang, Philippe Souères, Jian Li

Contact Dynamics and Coupled Stability of Massage Compliant Robotic Arm With Impedance Controller

Yuancan Huang[1,3], Philippe Souères[2] and Jian Li[3]

***Abstract*— The contact dynamics during massage manipulation by compliant robotic arm is described by using port-Hamiltonian modeling approach, which is a powerful tool for modeling complex dynamical systems due to the power port term. The nonlinear Hunt-Crossley model is used to replace the linear KelvinVoigt model in order to capture the behavior of soft tissues. Then, the impedance controller in [1], [2] is reformulated in full-state feedback form, and coupled stability is reassured form the energetic viewpoint. Some experiments are given to verify coupled stability during massage manipulation by compliant robotic arm.**

I. Introduction

Massage is a world-popular activity for relaxing muscles, relieving stress and improving the circulation, but usually laborious, time-consuming and short of experienced practitioners. Robots are naturally used to automate massage manipulation. Kume *et al*. [3] designed a massage robot with two end-effectors to implement the repetitive action of grasping on soft tissues. Jones *et al*. [4] showed that the ring and linear kneading manipulation can be realized by PUMA 562. Koga *et al*. [5], [6] developed an oral rehabilitation robot stimulating the maxillofacial tissues via rotational movements. In order to have both good performance and safety, an integrated rotary compliant joint is designed [7], and thus a 4-DOF anthropomorphic complaint arm is developed for the traditional Chinese medicine remedial massage [8] by the authors.

Impedance control and its variants are used by all massage robots in the literature in spite of the criticism on its performance and possible failure [9], [10], for they can guarantee the stable interaction with an unknown environment [11], [12]. However, knowledge on contact dynamics is instrumental in improving the performance of impedance control and exploring its limits [13], [14]. As our best knowledge, there is not yet the relevant works on this aspect for massage robots. We use the port-based network modeling approach, which has been recently developed to model complex dynamical systems[15], [16], to capture the contact dynamics during massage manipulation by the robotic arm with compliant joints. It describes a complex system in terms of port variables and the interconnection of systems via the ports by means of power continuity. The resulting network is mathematically described by a Dirac structure [17], which is a generalization of the Kirchhoff laws of circuit theory. The contribution of this work is threefold: the impedance control in [1], [2] is reformulated from the energetic viewpoints, and coupled stability is reassured in the port-Hamiltonian framework; we can improve the interacted behavior of impedance control with better knowledge on the human dynamics during massage manipulation; new control schemes by portinterconnection , such as IPC [18] and IDA-PBC [19], may be used for massage manipulation.

In this paper, the port-based network modeling approach is introduced in Section II, and rigid body kinematics and dynamics are briefly described in Section III. In Sections IV and V, contact kinematics and dynamics during massage manipulation are derived based on the port-Hamiltonian mechanism. Then, impedance controller is reformulated in full-state feedback form, and coupled stability is reassured form the energetic viewpoint in Section VI. Some experiments are given to verify coupled stability during massage manipulation in Section VII. Finally, Section VIII concludes, and discusses the further works on this research.

II. Port-based Network Modeling Approach

A. Mechanism on Port-based Network Modeling

In the Universe, dynamical behaviors of macrophysical systems are commonly constrained, either implicitly or explicitly, by the basic principles of physics, *i.e.*, energy conservation, positive entropy production, and power continuity. In terms of the first law of thermodynamics (*i.e.*, energy conservation law), energy can change forms, and can transfer from a system to another. But energy can be neither created nor annihilated. In the other hand, the second law of thermodynamics states that the entropy of an isolated system never decreases, because isolated systems spontaneously evolve toward thermodynamic equilibrium, *i.e.*, the state of maximum entropy. Or, to put it differently, the entropy of the system may decrease only due to a net energy flow out of the system, not by local annihilation. To sum up, there exist analogous basic behaviors with respect to energy in various physical domains, *i.e.*, storage, irreversible and reversible transformations, distribution and supply. Dy-

This work was supported by the National Natural Sciences Foundation of China under Research Grant 61075080

[1]Yuancan Huang is with the Institute of Intelligent Robot, School of Mechatronical Engineering, Beijing Institute of Technology, 100081 Beijing, China. Currently, he is a visiting researcher with Laboratoire d'Architecture et d'Analyse des Système, Centre National de la Recherche Scientifique (LAAS-CNRS), University of Toulouse, 31077 Toulouse, France yuancan.huang@laas.fr.

[2]Philippe Souères is with Laboratoire d'Architecture et d'Analyse des Système, Centre National de la Recherche Scientifique (LAAS-CNRS), University of Toulouse, 31077 Toulouse, France Philippe.Soueres@laas.fr.

[3]Jian Li is with the Institute of Intelligent Robot, School of Mechatronical Engineering, Beijing Institute of Technology, 100081 Beijing, China.

namical behaviors of physical systems can be modeled by describing energy flows among subsystems.

In computer science, the term ontology originated from metaphysics in philosophy is used as an efficient way formally representing knowledge as a set of concepts within a domain, and the relationships between pairs of concepts. With the analogous ideas, a systematic, meta-level, and object-oriented modeling approach, the port-based modeling network approach, has been developed for modeling complex, multi-domain physical systems, where each object is determined by constitutive relations on the one hand and its interface, being the power and signal ports to and from the external environment, on the other hand. Objects may be described in different levels and/or in different forms, but as long as the interface (number and type of ports) is unchanged, they can be interchanged in a straightforward manner. This allows top-down as well as bottom-up modeling and direct interconnection of (empty) submodels. Since empty submodel may be filled with specific description with various degrees of complexity (*i.e.*, models can be polymorphic), evolutionary and iterative modeling and design approaches are supported. Additionally, submodels may be constructed from other submodels resulting in hierarchical structures.

B. Dirac Structure and Port-Hamiltonian System

1) Dirac Structure: Let $\mathscr{F}\times\mathscr{F}^*$ denote the space of power variables, with $\mathscr{F}$ being an n-dimensional linear space, which is the space of flows (*e.g.*, velocities in mechanical domain and currents in electrical domain), and $\mathscr{F}^*$ being its dual, which is the space of efforts (*e.g.*, forces in mechanical domain and voltages in electrical domain), and let the dual product $\langle \boldsymbol{e},\boldsymbol{f}\rangle$ denote the power associated with the port $(\boldsymbol{e},\boldsymbol{f})\in\mathscr{F}\times\mathscr{F}^*$.

Definition 2.1: A (constant) Dirac structure on $\mathscr{F}$ is a linear subspace $\mathscr{D}\subset\mathscr{F}\times\mathscr{F}^*$ such that $\mathscr{D}=\mathscr{D}^\perp$ with $\perp$ the orthogonal complement with respect to $\langle\cdot,\cdot\rangle$, or, equivalently, $\dim\mathscr{D}=\dim\mathscr{F}$ and $\langle \boldsymbol{e},\boldsymbol{f}\rangle=0,\forall(\boldsymbol{e},\boldsymbol{f})\in\mathscr{D}$.

Remark 2.2: The condition implies that, if each pair $(\boldsymbol{e},\boldsymbol{f})$ belongs to the Dirac structure, or satisfies the network constraints, then $\langle \boldsymbol{e},\boldsymbol{f}\rangle=0$, *i.e.*, the sum of instantaneous powers passing through the port equals zero, which is nothing else than the Tellegen's theorem. This will lead to a rigorous description of a network structure which can be directly used for analysis.

Every Dirac structure $\mathscr{D}$ admits a kernel representation. Given a basis $\boldsymbol{f}_1,\dots,\boldsymbol{f}_n$ in $\mathscr{F}$, the corresponding dual basis $\boldsymbol{e}_1,\dots,\boldsymbol{e}_n$ in $\mathscr{F}^*$, and any basis in $\mathscr{U}$, with $\dim\mathscr{U}=m\geq n$, the linear maps F and E are represented by $m\times n$ matrices (which we denote by the same symbol as the maps) satisfying

$$\begin{aligned} EF^T+FE^T &= 0,\\ \mathrm{rank}[F|E] &= n. \end{aligned}$$

2) Port-Hamiltonian System: Consider a lumped-parameter physical system defined on a manifold M, with local coordinates $\boldsymbol{x}\in\mathbb{R}^n$. The total energy of the system is given by the Hamiltonian $H(\boldsymbol{x})$, and the system is assumed to have m boundary ports. For each $\boldsymbol{x}\in M$ we consider $\mathscr{F}_x=T_xM\times\mathbb{R}_m$ and $\mathscr{F}_x^*=T_x^*M\times\mathbb{R}_m$, and define a Dirac structure $\mathscr{D}(\boldsymbol{x})\subset\mathscr{F}_x\times\mathscr{F}_x^*$.

The flow variables of energy-storing elements are given as $\dot{\boldsymbol{x}}(t)$ and its effort variables as $\frac{\partial H}{\partial \boldsymbol{x}}(\boldsymbol{x}(t))$, which implies that $\langle\frac{\partial H}{\partial \boldsymbol{x}}(\boldsymbol{x}(t))\dot{\boldsymbol{x}}(t)\rangle=\frac{dH}{dt}(\boldsymbol{x}(t))$ is the increase in energy. In order to have a consistent sign convention that energy flows from the boundary ports into the system and from the internal network into the energy storing elements, let $\boldsymbol{f}_x=-\dot{\boldsymbol{x}}$ and $\boldsymbol{e}_x=\frac{\partial H}{\partial \boldsymbol{x}}$. In addition, $\boldsymbol{f}_b$ and $\boldsymbol{e}_b$ are power variables associated to the m boundary ports.

An implicit port-Hamiltonian system on M is defined by the set of differential and algebraic equations (DAE):

$$\left(-\dot{\boldsymbol{x}},\boldsymbol{f}_b,\frac{\partial H}{\partial \boldsymbol{x}},\boldsymbol{e}_b\right)\in\mathscr{D}(\boldsymbol{x}),\ \forall\boldsymbol{x}\in M$$

with the power-conservation property

$$0=\langle \boldsymbol{e},\boldsymbol{f}\rangle=\langle \boldsymbol{e}_x,\boldsymbol{f}_x\rangle+\langle \boldsymbol{e}_b,\boldsymbol{f}_b\rangle=-\frac{\partial H}{\partial \boldsymbol{x}}\dot{\boldsymbol{x}}+\boldsymbol{e}_b^T\boldsymbol{f}_b$$

from which $\frac{dH}{dt}=\boldsymbol{e}_b^T\boldsymbol{f}_b$.

Obviously, source or dissipative terms can be added to the system through the boundary ports.

Consider a kernel representation of an IPHS:

$$F(\boldsymbol{x})\begin{pmatrix}-\dot{\boldsymbol{x}}\\ \boldsymbol{f}_b\end{pmatrix}+E(\boldsymbol{x})\begin{pmatrix}\frac{\partial H}{\partial x}\\ \boldsymbol{e}_b\end{pmatrix}=0.$$

Assume that F and E can be split (non necessarily in a unique way) as

$$F=(F_x\ F_{b_1}\ F_{b_2}),\ E=(E_x\ E_{b_1}\ E_{b_2})$$

with $\mathrm{rank}\ F_x=n$ and $\mathrm{rank}\ (F_x\ F_{b_1}\ E_{b_2})=n+m$.

Let $\tilde{F}=(F_x\ F_{b_1}\ E_{b_2})$, $\tilde{E}=(E_x\ E_{b_1}\ F_{b_2})$, $\boldsymbol{y}=(\boldsymbol{f}_{b_1}^T\ \boldsymbol{e}_{b_2}^T)^T$, and $\boldsymbol{u}=(\boldsymbol{e}_{b_1}^T\ \boldsymbol{f}_{b_2}^T)^T$.

We have

$$\tilde{F}\begin{pmatrix}-\dot{\boldsymbol{x}}\\ \boldsymbol{y}\end{pmatrix}+\tilde{E}\begin{pmatrix}\frac{\partial H}{\partial x}\\ \boldsymbol{u}\end{pmatrix}=0$$

with $\tilde{F}\tilde{E}^T+\tilde{E}\tilde{F}^T=0$ and $\tilde{F}$ is invertible.

Premultiplying $\tilde{F}^{-1}$ on both sides, there is

$$\begin{pmatrix}-\dot{\boldsymbol{x}}\\ \boldsymbol{y}\end{pmatrix}=-\tilde{F}^{-1}\tilde{E}\begin{pmatrix}\frac{\partial H}{\partial x}\\ \boldsymbol{u}\end{pmatrix},$$

where $\tilde{F}^{-1}\tilde{E}$ is skew-symmetric because $\tilde{F}\tilde{E}^T+\tilde{E}\tilde{F}^T=0$, which is rewritten as

$$\tilde{F}^{-1}(\boldsymbol{x})\tilde{E}(\boldsymbol{x})=\begin{pmatrix}J(\boldsymbol{x}) & \boldsymbol{g}(\boldsymbol{x})\\ -\boldsymbol{x}^T(\boldsymbol{x}) & -B(\boldsymbol{x})\end{pmatrix},$$

with g arbitrary and J and B both skew-symmetric.

Finally, we obtain an explicit input/output PHS [15]:

$$\begin{aligned}\dot{\boldsymbol{x}} &= J(\boldsymbol{x})\frac{\partial H}{\partial \boldsymbol{x}}+g(\boldsymbol{x})\boldsymbol{u},\\ \boldsymbol{y} &= g(\boldsymbol{x})^T\frac{\partial H}{\partial \boldsymbol{x}}+B(\boldsymbol{x})\boldsymbol{u}.\end{aligned}$$

III. Rigid Body Kinematics and Dynamics

The motion of a rigid body can be described by the special Euclidean group $SE(3)$, whose element denoted the rigid body transformation relative to the reference frame. Let A be the reference frame and B the body frame. The element in the group $SE(3)$ may be represented by a homogeneous matrix of the form

$$T_b^a = \begin{pmatrix} R_b^a & \boldsymbol{p}_b^a \\ 0 & 1 \end{pmatrix},$$

where R_b^a is the rotation matrix of the body, belonging to the special orthogonal group $SO(3)$, and $\boldsymbol{p}_b^a$ the position vector of the origin of body frame.

The instantaneous velocity of a body with the frame B relative to another body with the frame C with respect to the reference frame A can be represented by a twist $\boldsymbol{t}_{b,c}^a$ of the form:

$$\boldsymbol{t}_b^{a,c} = \begin{bmatrix} \omega_b^{a,c} \\ \boldsymbol{v}_b^{a,c} \end{bmatrix},$$

where $\omega_b^{a,c}$ denotes the angular velocity of the body B relative to the body C with respect to the frame A, and $\boldsymbol{v}_b^{a,c}$ the linear velocity (relative to the frame C) of the fixed point in the frame B, that passes through the origin of the frame A.

A generalized force acting on a rigid body consists of a linear component (pure force) $\boldsymbol{f}$ and an angular component (pure moment) τ acting at a point, which is usually expressed by the wrench of the body with the frame B with respect to the reference frame A:

$$\boldsymbol{w}_b^a = \begin{bmatrix} \boldsymbol{f}_b^a \\ \tau_b^a \end{bmatrix}.$$

The adjoint representation of a Lie group is indicated with $Ad_{T_b^a}$:

$$Ad_{T_b^a} = \begin{pmatrix} R_b^k & \hat{\boldsymbol{p}}_b^a R_b^a \\ 0 & R_b^a \end{pmatrix},$$

which transforms twists from the frame B to the frame K, *i,e.*,

$$\boldsymbol{t}_c^{k,b} = Ad_{T_b^k} \boldsymbol{t}_c^{b,b}.$$

The duality $Ad_{T_b^k}^T$ transforms wrenches from the frame K to the frame B, *i,e.*,

$$\boldsymbol{w}_c^k = Ad_{T_b^k}^T \boldsymbol{w}_c^b.$$

IV. Contact Kinematics During Massage Manipulation

A. Gauss Map

In differential geometry, the Gauss map maps locally a surface in Euclidean space $\mathbb{R}^3$ to the unit sphere $\mathbb{S}^2$, *i.e.*, given a surface X embedded in $\mathbb{R}^3$, the Gauss map is a continuous map $\boldsymbol{n} : X \to \mathbb{S}^2$ such that $\boldsymbol{n}(p)$ is a unit vector orthogonal to X at p, the normal vector to X at p. The Gauss map can be defined globally if and only if the surface is orientable. The Jacobian determinant of the Gauss map is equal to Gaussian curvature. Its differential of the Gauss map is called the shape operator.

If X is orientable and smooth, then $\boldsymbol{n}(p)$ is well-defined and smooth over X. Hence a derivative mapping $\boldsymbol{n}_* : TX \to T\mathbb{S}^2$ can be defined. This implies that, while a point move tangentially on the surface X at the velocity $\boldsymbol{v} \in TX$, then the normal vector varies at the velocity $\boldsymbol{n}_*\boldsymbol{v} \in T\mathbb{S}^2$. Since the vector $\boldsymbol{n}(p)$ is commonly orthogonal to the surface X at p and the sphere $\mathbb{S}^2$ at $\boldsymbol{n}(p)$, an element $\boldsymbol{n}_*\boldsymbol{v} \in T\mathbb{S}^2$ can be mapped directly as an element $P\boldsymbol{n}_*\boldsymbol{v} \in T_pX$, where P is the linear mapping from $T_{\boldsymbol{n}(p)}\mathbb{S}^2$ to T_pX.

If $\boldsymbol{n}_*(p)\boldsymbol{v} = 0$ for all $\boldsymbol{v} \in T_pX$, then the surface X is locally flat at p. If $\langle \boldsymbol{v}, P\boldsymbol{n}_*\boldsymbol{v} \rangle > 0$ for all $\boldsymbol{v} \in T_pX$, then the surface X is locally convex at p.

B. Contact Kinematics During Massage Manipulation

For sake of kinematic analysis, the massage head and the human body are treated as two rigid bodies with the smooth, orientable surfaces X_1 and X_2, whose the Gauss maps are, respectively, defined as $\boldsymbol{n}_1$ and $\boldsymbol{n}_2$. As a result, the contact kinematics is amounted to the motion between two points p_1 and p_2 on the surfaces X_1 and X_2 with the shortest distance. Under the convexness assumptions, there are always such two unique points p_1 and p_2 in the boundary $X_1 \cup X_2)$ whose linking line l_n is normal to both the surfaces X_1 and X_2. Given a point $c \in l_n$ (e.g., the desired contact point), there is a unique plane O orthogonal to l_n and passing through the point c, as shown in Fig.1.

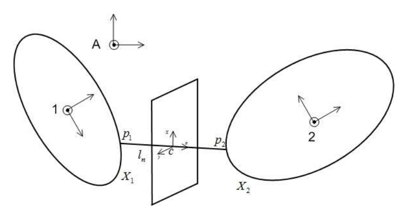

Fig. 1: Two points on X_1 and X_2 with the shortest distance.

Let $\boldsymbol{p}_i,\ i = 1, 2$, denote the position vector of the point p_i in its own frames 1 and 2. A minimum sign distance $\triangle \in \mathbb{R}$ is defined as:

$$\triangle = \langle \boldsymbol{n}_2, T_2^1 \boldsymbol{p}_1 - \boldsymbol{p}_2 \rangle.$$

If $\triangle > 0$, there is a distance $\triangle > 0$ between the bodies; otherwise, the bodies have a maximum penetration distance of $|\triangle|$ for $\triangle < 0$ or the contact for $\triangle = 0$. Here, a geometric description of the bodies is assume to be inflexible. This means that the two bodies are allowed to intersect virtually.

The velocities of p_1 and p_2 are uniquely determined by the following equations [20]:

$$\begin{aligned} \left[\boldsymbol{n}_{1*} + T_2^1 \boldsymbol{n}_{2*} T_1^2 (I + \triangle \boldsymbol{n}_{1*})\right] \dot{\boldsymbol{p}}_2 &= \hat{\boldsymbol{t}}_2^{1,1} + T_2^1 \boldsymbol{n}_{2*} (\dot{\triangle} \boldsymbol{n}_2 - \hat{\boldsymbol{t}}_1^{2,2} \boldsymbol{p}_2) \\ \left[\boldsymbol{n}_{2*} + T_1^2 \boldsymbol{n}_{1*} T_2^1 (I + \triangle \boldsymbol{n}_{2*})\right] \dot{\boldsymbol{p}}_1 &= \hat{\boldsymbol{t}}_1^{2,2} + T_1^2 \boldsymbol{n}_{1*} (\dot{\triangle} \boldsymbol{n}_1 - \hat{\boldsymbol{t}}_2^{1,1} \boldsymbol{p}_1), \end{aligned}$$

where $\hat{\boldsymbol{t}}_2^{1,1} = -T_2^1 \hat{\boldsymbol{t}}_1^{2,2} T_1^2$ can be any relative twist of the two bodies, $\dot{\triangle} = \langle \boldsymbol{n}_2, \hat{\boldsymbol{t}}_1^{2,2} T_1^2 \boldsymbol{p}_1 \rangle$, and $\triangle > \triangle_{\min}$ for some $\triangle_{\min} < 0$, which depends on the physical property of two bodies.

V. Contact Dynamics During Massage Manipulation

A. Hunt-Crossley Model

The soft tissues on the human body exhibit viscoelasticity. The simplest model characterized viscoelasticity is known as the Kelvin-Voigt model, which is represented by the parallel of a linear spring and a viscous damper. However, the linear model is not suitable to describe the behavior of human tissues, for viscous effects are substantial [21], [13]. Hunt and Crossley [22] showed that it is possible to obtain a behavior that is in better agreement with the physical intuition if the damping coefficient is made dependent on the body's relative penetration:

$$f(t) = \begin{cases} kd^n(t) + \lambda d^n(t)\dot{d}(t) & d \geq 0 \\ 0, & d < 0 \end{cases}$$

where the exponent n is a real number, usually close to unity, that takes into account the geometry of contact surfaces. Indeed, since the contact surface increases as the penetration depth $d(t)$ increases, the exponent allows taking into account the stiffness variation due to a larger contact area.

Moreover, the Hunt-Crossley model is consistent with the notion of coefficient of restitution used to characterize energy loss during impacts and, even if nonlinear, retains a certain computational simplicity. Beside these properties, it is important to note that the physical consistency of the model can be preserved by a proper generalization to the full geometrical contact description [six degrees of freedom (DOF)], as discussed in [23], [24]. Therefore, we can use a spatial spring in parallel with a spatial damper to describe soft tissues.

B. Port-Based Network Description for Massage Manipulation

During massage manipulation, one is asked to sit on a chair or to lie on a bed, to keep relaxed and steady as far as possible, and not to actively exert any force back. It is reasonable that the human body in massage manipulation is modeled as an inertial mass with a spatial spring and damper, representing the viscoelastic property of soft tissues, and a spatial spring, representing the reaction force on the robotic arm from the chair or the bed, or by one who tries to keep his body steady, see Fig. 2.

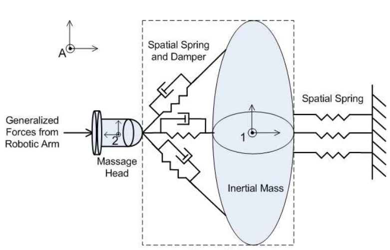

Fig. 2: Dynamical description for massage manipulation.

From the view point of port-based network modeling, a contact Dirac structure may be used to interconnect the robotic arm, the inertial mass with a spatial spring representing the human body with some kinematic constraints, the storage elements representing elastic effect of soft tissue, and the dissipation elements representing viscous effect of soft tissue and Coulomb friction. Optionally, one control port can be added to regulate the behaviors of the robotic arm. Figure 3 shows the interconnection structure of port-based model of massage manipulation.

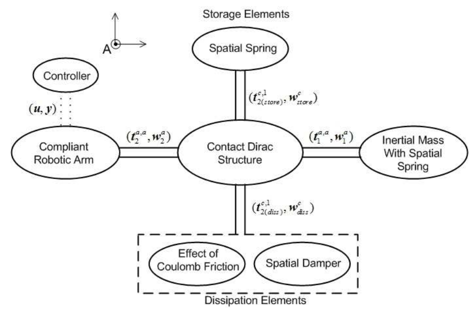

Fig. 3: Interconnection structure of port-based model.

C. Contact Dynamics During Massage Manipulation

1) Contact Dirac Structure: Define the binary signal $s_{\triangle}$ as

$$s_{\triangle} = \begin{cases} 1, & \text{if } \triangle \geq 0, \\ 0, & \text{otherwise.} \end{cases}$$

Then, $s_{\triangle} = 1$ if there is no contact and $s_{\triangle} = 0$ if there is contact.

Here, we only consider the massage manipulations without rolling on the human body. Hence the motion can be decomposed into two terms involving rolling or not. A set of basis velocity screws of $se(3)$ are chosen as two screws (r_x, r_y) representing the pure rotations around two axis lying on O and passing through c, and the others (t_x, t_y, t_z, r_z) the three translations and the pure rotation around l_n, as shown in Fig.1. Now $se(3)$ has the following decomposition:

$$se(3) = R_{xy} \oplus (se(2) \times T_z),$$

where $R_{xy} := span\{r_x, r_y\}$ and the Lie algebra $se(2) \times T_z$ represents the motions on $O(se(2))$ together with the normal translation along $l_n(T)$.

Define a projection operator $P_{se(2)\times T_z} : se(3) \to se(2) \times T_z$. It can be represented by the matrix P while the coordinate system is selected. Its adjoint operator $P^*_{se(2)\times T_z} : (se(2) \times T_z)^* \to se^*(3)$ maps the wrench $\boldsymbol{w}^c_{2,1} \in (se(2) \times T_z)^*$ into the wrench $P^T \boldsymbol{w}^c_{2,1} \in se^*(3)$, the sum of the wrenches from the spatial spring and damper as well as the friction effect.

The Dirac structure with the desired ports $(\boldsymbol{t}^{a,a}_1, \boldsymbol{w}^a_1)$, $(\boldsymbol{t}^{a,a}_2, \boldsymbol{w}^a_2)$, $(\boldsymbol{t}^{c,1}_{2(store)}, \boldsymbol{w}^c_{store})$ and $(\boldsymbol{t}^{c,1}_{2(diss)}, \boldsymbol{w}^c_{diss})$ is given as[24]:

$$E \begin{pmatrix} \boldsymbol{w}^a_1 \\ \boldsymbol{w}^a_2 \\ \boldsymbol{w}^c_{store} \\ \boldsymbol{w}^c_{diss} \end{pmatrix} + F \begin{pmatrix} \boldsymbol{t}^{a,a}_1 \\ \boldsymbol{t}^{a,a}_2 \\ \boldsymbol{t}^{c,1}_{2(store)} \\ \boldsymbol{t}^{c,1}_{2(diss)} \end{pmatrix} = 0$$

with

$$E := \begin{pmatrix} I_6 & 0 & (s_\triangle - 1)Ad^T_{T^c_a}P^T & (s_\triangle - 1)Ad^T_{T^c_a}P^T \\ 0 & I_6 & (1-s_\triangle)Ad^T_{T^c_a}P^T & (1-s_\triangle)Ad^T_{T^c_a}P^T \\ 0 & 0 & 0 & 0 \\ 0 & 0 & 0 & 0 \end{pmatrix}$$

and

$$F := \begin{pmatrix} 0 & 0 & 0 & 0 \\ 0 & 0 & 0 & 0 \\ (s_\triangle - 1)PAd_{T^c_a} & (s_\triangle - 1)PAd_{T^c_a} & -I_4 & 0 \\ (s_\triangle - 1)PAd_{T^c_a} & (s_\triangle - 1)PAd_{T^c_a} & 0 & -I_4 \end{pmatrix},$$

where the switching element in E is used to switch off the contact forces $\boldsymbol{w}^c_{store}$ and $\boldsymbol{w}^c_{diss}$ while no contact occurs. Since the matrix F and E satisfy the rank condition, the power continuity condition $EF^T + FE^T = 0$ holds for all values of $s_\triangle$.

The connection of the storage and dissipation elements depends on whether the contact occurs or not, thus the Dirac structure is time-varying.

2) Compliant Robotic Arms: As shown in Fig. 4, the serial elasticity in the ith compliant rotary joint is modeled as a linear torsional spring with stiffness k_i. Due to the extra degrees of freedom introducing by the serial elasticity between the motor shaft and the link, the motor rotor (including gear) has to be modeled by a fictitious link with its own inertia I^r_i. Thereby we can regard that an n-link compliant robotic arm consists of n actual links and n fictitious links [25].

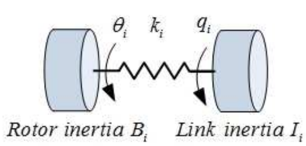

Fig. 4: Diagram of the i-th compliant joint

Assume that the the rotor inertia is symmetric with respect to the rotor axis of rotation so that the gravitational potential and also the velocity of the rotor center of mass are both independent of the rotor angular position. Normally, this assumption hardly needs to be justified, for it is a norm in robot design.

Let $\boldsymbol{q} = (q_1, \dots, q_n)^T$ and $\theta = (\theta_1, \dots, \theta_n)^T$ be the generalized coordinates for an n-link compliant robotic arm where q_i and θ_i, respectively, represent the angles of the link i and the rotor i, $i = 1, \dots, n$.

The kinetic energy of the ith rotor is

$$T^r_i = \frac{1}{2}m_i(\boldsymbol{v}^r_i)^T\boldsymbol{v}^r_i + \frac{1}{2}\dot{\theta}^T_i B_i \dot{\theta}_i, \tag{1}$$

where $\boldsymbol{v}^r_i$ denotes the velocity of the center of mass of the rotor, m_i the rotor mass, and B_i the inertia of the rotor. Now by the symmetry assumption of the rotor the velocity $\boldsymbol{v}^r_i$ only depends on the link variables $q_1, \dots, q_{i-1}$. Thus if the rotor mass is included as a part of the link $i-1$ to calculate its inertia tensor then the first term in (1) will be absorbed in the translational kinetic energy of the link $i-1$.

We have shown that the total kinetic energy of an n-link compliant robotic arm under the symmetry assumption is composed of two parts: the kinetic energy of the rigid robotic arm where we neglect the elasticity in the joint, and the rotational kinetic energy of the rotors, namely

$$T(\boldsymbol{q}, \theta, \dot{\boldsymbol{q}}, \dot{\theta}) = \frac{1}{2}\dot{\boldsymbol{q}}^T M(\boldsymbol{q})\boldsymbol{q} + \frac{1}{2}\dot{\theta}^T B \dot{\theta}, \tag{2}$$

where $M(\boldsymbol{q})$ is the inertia matrix of the rigid robotic arm, which can be calculated using standard techniques once the rotor masses are regarded as a part of the proximal links for calculating their inertia tensor, and B the inertia matrix of the rotors.

Next, the elastic potential of the spring is given as

$$P(\boldsymbol{q}, \theta) = \frac{1}{2}(\boldsymbol{q} - \theta)^T K(\boldsymbol{q} - \theta),$$

where K is a diagonal matrix whose diagonal elements are the spring stiffness coefficients. Invoking again the symmetry assumption, the gravitational potential is a function only of $\boldsymbol{q}$. Therefore, the total potential energy is

$$U(\boldsymbol{q}, \theta) = P(\boldsymbol{q}, \theta) + G(\boldsymbol{q}), \tag{3}$$

where the gravitational potential energy term $G(\boldsymbol{q})$ is found from the standard formulae for rigid robots.

The Lagrangian is

$$L(\boldsymbol{q}, \theta, \dot{\boldsymbol{q}}, \dot{\theta}) = T(\boldsymbol{q}, \theta, \dot{\boldsymbol{q}}, \dot{\theta}) - U(\boldsymbol{q}, \theta).$$

For sake of clarity, the generalized coordinates $\boldsymbol{q}$ and θ are rewritten as $\boldsymbol{q}_q$ and $\boldsymbol{q}_\theta$. Now the generalized momenta $\boldsymbol{p}_q$ and $\boldsymbol{p}_\theta$ are defined as

$$\begin{aligned} \boldsymbol{p}_q &= \frac{\partial L}{\partial \dot{\boldsymbol{q}}_q}, \\ \boldsymbol{p}_\theta &= \frac{\partial L}{\partial \dot{\boldsymbol{q}}_\theta}. \end{aligned}$$

By the Legendre transform of $L(\boldsymbol{q}_q, \boldsymbol{q}_\theta, \dot{\boldsymbol{q}}_q, \dot{\boldsymbol{q}}_\theta)$ as a function of $(\dot{\boldsymbol{q}}_q, \dot{\boldsymbol{q}}_\theta)$, it follows that the Hamiltonian function is

$$\begin{aligned} H_R(\boldsymbol{q}_q, \boldsymbol{q}_\theta, \boldsymbol{p}_q, \boldsymbol{p}_\theta) = {} & \frac{1}{2}\boldsymbol{p}^T_q M^{-1}(\boldsymbol{q}_q)\boldsymbol{p}_q + \frac{1}{2}\boldsymbol{p}^T_\theta B^{-1}\boldsymbol{p}_\theta \\ & + \frac{1}{2}(\boldsymbol{q}_q - \boldsymbol{q}_\theta)^T K(\boldsymbol{q}_q - \boldsymbol{q}_\theta) + G(\boldsymbol{q}_q). \end{aligned}$$

Hence, the Hamiltonian system of the compliant robotic arm are given as

$$\begin{aligned} \dot{\boldsymbol{q}}_q &= M^{-1}(\boldsymbol{q}_q)\boldsymbol{p}_q \\ \dot{\boldsymbol{q}}_\theta &= B^{-1}\boldsymbol{p}_\theta \\ \dot{\boldsymbol{p}}_q &= -\frac{1}{2}\boldsymbol{p}^T_q \frac{\partial M^{-1}(\boldsymbol{q}_q)}{\partial \boldsymbol{q}_q}\boldsymbol{p}_q - K(\boldsymbol{q}_q - \boldsymbol{q}_\theta) - \boldsymbol{g}(\boldsymbol{q}_q) \\ \dot{\boldsymbol{p}}_\theta &= K(\boldsymbol{q}_q - \boldsymbol{q}_\theta), \end{aligned}$$

where $\boldsymbol{g}(\boldsymbol{q}_q) = \frac{G(\boldsymbol{q}_q)}{\partial \boldsymbol{q}_q}$.

Assume that $\boldsymbol{t}^{a,a}_2 = J_R(\boldsymbol{q}_q)\dot{\boldsymbol{q}}_q$ where $J(\boldsymbol{q}_q)$ is the Jacobian of the rigid robotic arm. Its dual relation is $\tau_{ext} = J^T_R(\boldsymbol{q}_q)\boldsymbol{w}^a_2$ where

τ_{ext} represents the external torque acting on the end-effector of robotic arm. If one control port $(\boldsymbol{u},\boldsymbol{y})$ and one interacted port $(\boldsymbol{t}_2^{a,a},\boldsymbol{w}_2^a)$ are attached, we obtain a port-Hamiltonian system with two ports, written in more compact form:

$$\begin{aligned}\begin{pmatrix}\dot{\boldsymbol{q}}_q\\ \dot{\boldsymbol{q}}_\theta\\ \dot{\boldsymbol{p}}_q\\ \dot{\boldsymbol{p}}_\theta\end{pmatrix} &= \begin{pmatrix}0&0&I_q&0\\0&0&0&I_\theta\\-I_q&0&0&0\\0&-I_\theta&0&0\end{pmatrix}\\ &\times\begin{pmatrix}M^{-1}(\boldsymbol{q}_q)\boldsymbol{p}_q\\ B^{-1}\boldsymbol{p}_\theta\\ \frac{1}{2}\boldsymbol{p}_q^T\frac{\partial M^{-1}(\boldsymbol{q}_q)}{\partial \boldsymbol{q}_q}\boldsymbol{p}_q+K(\boldsymbol{q}_q-\boldsymbol{q}_\theta)+\boldsymbol{g}(\boldsymbol{q}_q)\\ -K(\boldsymbol{q}_q-\boldsymbol{q}_\theta)\end{pmatrix}+\begin{pmatrix}0\\0\\0\\ \boldsymbol{u}\end{pmatrix}\\ &+\begin{pmatrix}0\\0\\J_R^T(\boldsymbol{q}_q)\boldsymbol{w}_2^a\\0\end{pmatrix}\\ \boldsymbol{y} &= -K(\boldsymbol{q}_q-\boldsymbol{q}_\theta)\\ \boldsymbol{t}_2^{a,a} &= J_R(\boldsymbol{q}_q)\dot{\boldsymbol{q}}_q,\end{aligned}$$

where $\boldsymbol{u}$ represents the motor torque vector.

3) Inertial Mass With Spatial Spring: The Hamiltonian of the inertial mass with spatial spring is

$$H_I(\boldsymbol{q}_I,\dot{\boldsymbol{q}}_I)=\frac{1}{2}\dot{\boldsymbol{q}}_I^T M_I(\boldsymbol{q}_I)\dot{\boldsymbol{q}}_I+\frac{1}{2}(\boldsymbol{q}_I-\boldsymbol{q}_I^0)^T K_I(\boldsymbol{q}_I)(\boldsymbol{q}_I-\boldsymbol{q}_I^0),$$

where $\boldsymbol{q}_I$ is the configuration vector, $M_I(\boldsymbol{q}_I)$ the inertia matrix, and $K_I(\boldsymbol{q}_I)$ the linear spatial spring stiffness matrix. $\boldsymbol{q}_I^0$ is some reference position.

Let $\boldsymbol{p}_I=M_I(\boldsymbol{q}_I)\dot{\boldsymbol{q}}_I$. The port-Hamiltonian equation with the port pair $(\boldsymbol{t}_1^{a,a},\boldsymbol{w}_1^a)$ is

$$\begin{aligned}\dot{\boldsymbol{q}}_I &= M_I^{-1}(\boldsymbol{q}_I)\boldsymbol{p}_I+J_I(\boldsymbol{q}_I)\boldsymbol{t}_1^{a,a},\\ \dot{\boldsymbol{p}}_I &= -\frac{1}{2}\boldsymbol{p}_I^T\frac{\partial M^{-1}(\boldsymbol{q}_I)}{\partial \boldsymbol{q}_I}\boldsymbol{p}_I-K_I(\boldsymbol{q}_I)(\boldsymbol{q}_I-\boldsymbol{q}_I^0)\\ &\quad -\frac{1}{2}(\boldsymbol{q}_I-\boldsymbol{q}_I^0)^T\frac{\partial K_I(\boldsymbol{q}_I)}{\partial_{\boldsymbol{q}_I}}(\boldsymbol{q}_I-\boldsymbol{q}_I^0),\\ \boldsymbol{w}_I &= J_I^T(\boldsymbol{q}_I)\boldsymbol{w}_1^a,\end{aligned}$$

where $J_I(\boldsymbol{q}_I)$ is the transformation matrix from the frame A to the frame in the inertial mass.

The energy balancing relation is

$$\frac{dH_I}{dt}=(\boldsymbol{w}_1^a)^T\boldsymbol{t}_1^{a,a}.$$

4) Viscoelastic Coupling Description and Coulomb friction: Normally, the massage head is made by ceramic material, which is much stiffer than the human body, and thus may be regraded as a rigid body. Therefore, the contact point c lies on the surface of the human body, and then the plane O is the tangent plane of the surface at c. As a contact frame C is defined, the deformation at time t is calculated as:

$$T(t)=\int_0^t \boldsymbol{t}_{2(store)}^{c,1}(\tau)T(\tau)d\tau.$$

Here, $T(t)$ is a 4×4 homogeneous matrix of the form

$$T(t)=\begin{pmatrix}\cos\theta & -\sin\theta & 0 & x\\ \sin\theta & \cos\theta & 0 & y\\ 0&0&1&z\\0&0&0&1\end{pmatrix}$$

where θ is the rotational angle around the line l_n.

The stiffness matrix on a manifold requires differentiation of the generalized force in the direction of the generalized velocity. Given a potential function Φ, the force one-form $\mathscr{F}$ is therefore:

$$\mathscr{F}=d\Phi.$$

Assume that the vectors $L_1,\ldots,L_4$ are basis for the Lie algebra $se(2)\times T$, the vectors $\hat{L}_1,\ldots,\hat{L}_4$ form a basis of the tangent space at any point $T\in SE(2)\times T$, where $\hat{L}_i$, $i=1,\ldots,4$, are the left invariant vector fields at T. In order to give the stiffness matrix, the manifold is endowed with an affine connection so that the covariant derivative, $\nabla_Y X$, of a vector field X with respect to a vector field Y may be defined. If X_i is a set of basis vector fields, there is

$$\nabla_{X_i}X_j=\Gamma_{ji}^k X_k,$$

where the coefficients Γ_{ji}^k are called Christoffel symbols.

Hence, the coefficients of the stiffness matrix $K_s\left(T_{2(store)}^{c,1}\right)$ are [26]

$$k_{ij}^s\left(T_{2(store)}^{c,1}\right)=\langle\nabla_{\hat{L}_i}dP_{spring};\hat{L}_i\rangle.$$

Finally, we have

$$\boldsymbol{w}_{store}^c=K_s\left(T_2^{c,1}\right)\delta\boldsymbol{t}_{2(store)}^{c,1},$$

where $\delta\boldsymbol{t}_{2(store)}^{c,1}$ represents the variation of the twist $\boldsymbol{t}_{2(store)}^{c,1}$.

Likewise, the dissipative parts are expressed in the form:

$$\boldsymbol{w}_{diss}^c=D_d\left(\delta\boldsymbol{t}_{2(diss)}^{c,1}\right)\boldsymbol{t}_{2(diss)}^{c,1}+K_f\boldsymbol{t}_{2(diss)}^{c,1},$$

where $D_d\left(\delta\boldsymbol{t}_{2(diss)}^{c,1}\right)$ is the damping matrix defined by the Rayleigh function R_{damper} in the way that $\boldsymbol{w}_{damper}^c=\frac{\partial R_{damper}}{\partial \boldsymbol{t}_{2(diss)}^{c,1}}$, and K_f is the constant friction coefficient matrix. Here, only kinetic friction is considered.

The total energy of the viscoelastic and friction parts is

$$H_V=P_{spring}+R_{damper}+R_{fric}$$

with

$$R_{fric}=\frac{1}{2}\left(\boldsymbol{t}_{2(diss)}^{c,1}\right)^T K_f\boldsymbol{t}_{2(diss)}^{c,1}.$$

VI. Impedance Controller and Coupled Stability

A. Impedance Controller

From the energy shaping viewpoints, an impedance controller with two feedback loops is constructed in [1], [2]. Rewritten in the matrix form, the torque inner loop is

$$\boldsymbol{u}=BB_a^{-1}\boldsymbol{v}+(I-BB_a^{-1})K(\boldsymbol{q}_q-\boldsymbol{q}_\theta)+DK^{-1}(\dot{\boldsymbol{q}}_q-\dot{\boldsymbol{q}}_\theta),\quad (4)$$

where $\boldsymbol{v}$ is an intermediate control input vector, B_a the motor apparent inertia vector with respect to $\boldsymbol{v}$, and D the desired damping matrix.

The impedance outer loop is a PD controller with gravity compensation:

$$\boldsymbol{v} = -K_q(\boldsymbol{q}_q - \boldsymbol{q}_q^d) - D_q\dot{\boldsymbol{q}}_q + \boldsymbol{g}(\boldsymbol{q}_q), \tag{5}$$

where $\boldsymbol{q}_q^d$ is the desired rotor angular position vector.

Obviously, the impedance controller is a full-state feedback controller. Unfortunately, the control law (5) does not satisfy the required passivity condition. A solution is to choose $\boldsymbol{v}$ as a function of $\boldsymbol{q}_\theta$ and its derivative $\dot{\boldsymbol{q}}_\theta$ by replacing $\boldsymbol{q}_q$ with its stationary equivalent to $\hat{\boldsymbol{q}}_q(\boldsymbol{q}_\theta)$, namely:

$$\boldsymbol{v} = -K_q(\hat{\boldsymbol{q}}_q(\boldsymbol{q}_\theta) - \boldsymbol{q}_q^d) - D_q\dot{\hat{\boldsymbol{q}}}_q(\boldsymbol{q}_\theta) + \boldsymbol{g}(\hat{\boldsymbol{q}}_q(\boldsymbol{q}_\theta)), \tag{6}$$

In the sufficiently small neighborhood of the equilibrium point, $\hat{\boldsymbol{q}}_q(\boldsymbol{q}_\theta)$ can be solved from

$$\boldsymbol{q}_\theta = \boldsymbol{f}(\boldsymbol{q}_q) = \boldsymbol{q}_q + K^{-1}[-K_q(\boldsymbol{q}_q - \boldsymbol{q}_\theta) + \boldsymbol{g}(\boldsymbol{q}_q)].$$

Generally, the inverse function $\boldsymbol{f}^{-1}$ has not analytic expression. For a given $\boldsymbol{q}_\theta$, it is possible to approximate the value $\hat{\boldsymbol{q}}_q(\boldsymbol{q}_\theta) = \boldsymbol{f}^{-1}(\boldsymbol{q}_\theta)$ with arbitrary precision by iteration method.

Due to gravity compensation and propositional terms in the controller, the Hamiltonian of the closed-loop system is

$$H_R^c(\boldsymbol{q}_q,\boldsymbol{q}_\theta,\boldsymbol{p}_q,\boldsymbol{p}_\theta) = \frac{1}{2}\boldsymbol{p}_q^T M^{-1}(\boldsymbol{q}_q)\boldsymbol{p}_q + \frac{1}{2}\boldsymbol{p}_\theta^T B_a^{-1}\boldsymbol{p}_\theta + \frac{1}{2}(\boldsymbol{q}_q - \boldsymbol{q}_\theta)^T K(\boldsymbol{q}_q - \boldsymbol{q}_\theta) + \frac{1}{2}(\boldsymbol{q}_q - \boldsymbol{q}_q^d)^T K(\boldsymbol{q}_q - \boldsymbol{q}_q^d).$$

It has been shown [] that, for the robots only with rotational joints, there is

$$\begin{aligned} \frac{dH_R^c}{dt} &= -\dot{\boldsymbol{q}}_\theta^T D_q \dot{\boldsymbol{q}}_\theta - (\dot{\boldsymbol{q}}_\theta - \dot{\boldsymbol{q}}_q)^T D(\dot{\boldsymbol{q}}_\theta - \dot{\boldsymbol{q}}_q) + (\boldsymbol{w}_2^a)^T \boldsymbol{t}_2^{a,a} \\ &< (\boldsymbol{w}_2^a)^T \boldsymbol{t}_2^{a,a}, \end{aligned}$$

i.e., the overall closed system is strictly passive with respect to the port pair $(\boldsymbol{t}_2^{a,a}, \boldsymbol{w}_2^a)$. The compliant robotic arm with the impedance controller is a port-Hamiltonian system.

B. Coupled Stability

The Hamiltonian of the total interconnection systems is

$$H = H_R^c + H_I + H_V.$$

By their definition, we have evidently

$$\frac{dH}{dt} < 0, \qquad \forall s_\triangle.$$

In other words, the compliant robotic arm with impedance controller is asympotically stable no matter whether it contacts with the human body or not.

VII. Experimental Verification

To verify coupled stability, pressing, kneading, and plucking are realized on the human body by the 4-DOF anthropomorphic compliant robotic arm in two scenarios with sitting on a chair and lying on a bed, see Fig. 5. Their manipulation processes can be described as an up and down cyclic motion vertical to the surface of human body, a circular and rectilinear cyclic motions tangential to the surface of human body, respectively. All of three massage movements have a downward force on the human body. During massage manipulation process,

(a) Sitting scenario (b) Lying scenario

Fig. 5: Two scenarios for verifying coupled stability

force curves are measured by JR3 6DOF force-torque sensors 50M31. The experimental results in in Fig. 6 and Fig. 7 show that coupled stability is guaranteed during different interacted scenarios, as indicated by the foregoing theoretical analysis.

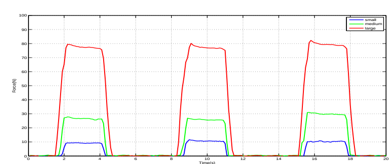

(a) Pressing

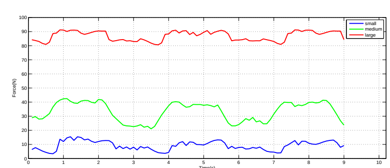

(b) Kneading

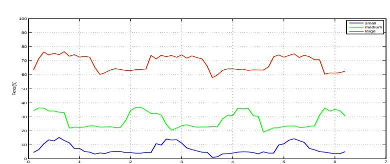

(c) Plucking

Fig. 6: Force curves of massage manipulation in lying scenario

VIII. Conclusions and Discussions

In this paper, the port-Hamiltonian modeling approach is used to model the massage manipulation by compliant robotic arm. Its use is substantiate three aspects: the impedance control for compliant robotic arm in [1], [2] is reformulated from the

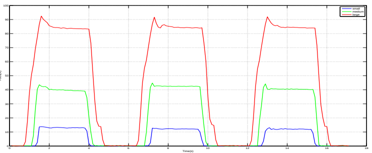

(a) Pressing

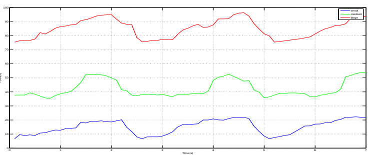

(b) Kneading

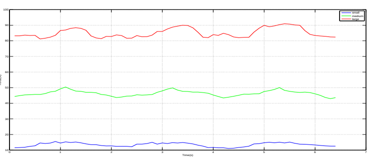

(c) Plucking

Fig. 7: Force curves of massage manipulation in sitting scenario

energetic viewpoints, and coupled stability is reassured in the port-Hamiltonian framework; it is possible to improve the interacted behavior of impedance control with better knowledge on the contact dynamics for massage manipulation; the control schemes by portinterconnection, which have been intensively studied in the literature, may be used for massage manipulation. Then, pressing, kneading, and plucking are realized on the human body by the 4-DOF anthropomorphic compliant robotic arm in two scenarios to verify the coupled stability during massage manipulation. The results show that coupled stability is guaranteed during different interacted scenarios, as indicated by the foregoing theoretical analysis.

In the future, we will use the contact dynamics to study the massage performance of impedance control, to explore the influence of the impedance variation, and to develop new control schemes and new model so that more complicated massage manipulation is realized, *e.g.*, rolling on the human body in which nonholonomic constraints must be considered, and tapping on the human body in which we need to describe impact dynamics.

IX. Acknowledgments

The authors gratefully appreciate the support of this research by the National Natural Sciences Foundation of China and reviewers' comments.

References

[1] C. O. A. Albu-Schäffer and G. Hirzinger, "A unified passivity-based control framework for position, torque and impedance control of flexible joint," *Int. J. Robot. Res.*, vol. 26, no. 1, pp. 23–39, 2007.

[2] A. K. C. Ott, A. Albu-Schäffer and G. Hirzinger, "On the passivity-based impedance control of flexible joint robots," *IEEE J. Robotics Auromat.*, vol. 24, no. 2, pp. 416–429, 2008.

[3] M. Kume and *et al.*, "Development of a mechanotherapy unit for examining the possibility of an intelligent massage robot," in *Proc. of IEEE/RSJ Int. Conf. on Intelligent Robots and Systems*, Osaka, 1996, pp. 346–353.

[4] K. Jones and D. Winncy, "Development of a massage robot for medical therapy," in *Proc. of IEEE/ASME Int. Conf. on Advanced Intelligent Mechatronics*, 2003, pp. 1096–1101.

[5] H. Koga and *et al.*, "Development of oral rehabilitation robot for massage therapy," in *Proc. of Int. Special Topic Conf. on ITAB*, Tokyo, 2007, pp. 111–114.

[6] ——, "Development of the oral rehabilitation robot wao-1," in *Proc. of IEEE RAS/EMBS Int. Conf. on Biomedical Robotics and Biomechatronics*, Scottsdale, AZ, 2008, pp. 556–561.

[7] Y. Huang and *et al.*, "Integrated rotary compliant joint and its impedance-based controller for single-joint pressing massage robot," in *Proc. of IEEE Int. Conf. on Robotics and Biomimetics*, Guangzhou, China, 2012, pp. 1962–1967.

[8] ——, "Design and control of anthropomorphic BIT soft arms for TCM remedial massage," in *Proc. of IEEE/RSJ Int. Conf. on Intelligent Robots and Systems*, Tokyo, 2013.

[9] T. Valency and M. Zacksenhouse, "Accuracy/robustness dilemma in impedance control," *ASME J. Dynam. Syst. Meas. Contr.*, vol. 125, pp. 310–319, 2003.

[10] B. S. S. Chiaverini and L. Villani, "A survey of robot interaction control schemes with experimental comparison," *IEEE/ASME Trans. on Mechatronics*, vol. 4, no. 3, pp. 273–285, 1999.

[11] N. Hogan, "On the stability of manipulators performing contact tasks," *IEEE J. Robot. Autom.*, vol. 4, no. 6, pp. 677–686, 1988.

[12] J. E. Colgate and N. Hogan, "Robust control of dynamically interacting systems," *Int. J. Control*, vol. 48, p. 6588, 1988.

[13] C. M. N. Diolaiti and S. Stramigioli, "Contact impedance estimation for robotic systems," *IEEE Trans. Robotics*, vol. 21, pp. 925–935, 2005.

[14] S. P. Buerger and N. Hogan, "Complementary stability and loop shaping for improved humanrobot interaction," *IEEE Trans. Robotics*, vol. 23, pp. 232–244, 2007.

[15] S. S. V. Duindam, A. Macchelli and H. B. (Eds.), *Modeling and Control of Complex Physical Systems-The Port-Hamiltonian Approach*. Berlin: Springer-Verlag, 2009.

[16] A. J. van der Schaft, *L_2-Gain and Passivity Techniques in Nonlinear Control (Communication and Control Engineering Series)*. Berlin, Germany: Springer-Verlag, 2000.

[17] M. Dalsmo and A. J. van der Schaft, "On representation and integrability of mathematical structures in energy-conserving physical systems," *SIAM J. Control Optim.*, vol. 37, p. 5491, 1999.

[18] A. J. van der Schaft, *Modeling and IPC Control of Interactive Mechanical Systems: A Coordinate Free Approach*. London, U.K.: Springer-Verlag, 2001.

[19] A. A. J. Acosta, R. Ortega and A. D. Mahindrakar, "Interconnection and damping assignment passivity-based control of mechanical systems with underactuation degree one," *IEEE Trans. on Automatic Control*, vol. 50, no. 12, pp. 1936–1955, 2005.

[20] V. Duindam and S. Stramigioli, "Modeling the kinematics and dynamics of compliant contact," in *Proc. of the 2003 IEEE International Conference on Robotics and Automation*, Taipei, Taiwan, 2003, pp. 4029–4034.

[21] G. Gilardi and I. Sharf, "Literature survey of contact dynamics modeling," *J. Mech. Mach. Theory*, vol. 37, no. 10, p. 12131239, 2002.

[22] K. Hunt and F. Crossley, "oefficient of restitution initerpreted as damping in vibroimpact," *ASME J. Appl. Mech.*, vol. 42, p. 440445, 1975.

[23] S. Stramigioli, "Modeling the kinematics and dynamics of compliant contact," in *Proc. 2nd Workshop Lagrangian, Hamiltonian Methods Nonlinear Control*, Sevilla, Spain, 2003, p. 1726.

[24] S. Stramigioli and V. Duindam, "Port based modeling of spatial viscoelastic contacts," *Eur. J. Control*, vol. 10, p. 510519, 2004.

[25] M. W. Spong, "Modeling and control of elastic joint robots," *ASME J. Dynam. Syst. Meas. Contr.*, vol. 109, no. 4, pp. 310–319, 1987.

[26] M. Zefran and V. Kumar, "Affine connections for the cartesian stiffness matrix," in *Proc. of the 1997 IEEE international conference on robotics and automation*, New Mexico, 1997, pp. 1376–1381.